Modeling the Vapor and Dust Dynamics Due to the Impact of the LCROSS Spacecraft on the Moon

D. B. Goldstein, D. Summy, A. Colaprete, P. L. Varghese, and L. M. Trafton

Citation: AIP Conference Proceedings **1084**, 1061 (2008); doi: 10.1063/1.3076439
View online: http://dx.doi.org/10.1063/1.3076439
View Table of Contents: http://scitation.aip.org/content/aip/proceeding/aipcp/1084?ver=pdfcov
Published by the AIP Publishing

Modeling the Vapor and Dust Dynamics Due to the Impact of the LCROSS Spacecraft on the Moon.

D. B. Goldstein[1], D. Summy[1], A. Colaprete[2], P. L. Varghese[1], L. M. Trafton[1]

[1] *U. Texas at Austin, TX,* [2] *NASA Ames Research Center, Moffett Field, CA*

Abstract. The implications of possibly large volatile reservoirs on the Moon are significant for the future of manned activity there and for space science and exploration in general. In autumn of 2008 NASA will launch the LCROSS mission to impact two spacecraft into a permanently shadowed crater – a cold trap - at the south pole of the Moon. The lead spacecraft will excavate its own several meter crater. The process will be observed by the following smaller vehicle and by orbiting and Earth-based instruments in hopes of observing the release of volatiles -- predominantly water -- from the lunar soil. The following vehicle will then impact as well. We examine the plausible vapor dynamics following the impacts and concentrate on the observability of the gas from Earth or lunar orbit. In the free-molecular computational model of the vapor motion, water and OH molecules move ballistically, have a temperature-dependent surface residence time, and are subject to photo-dissociation and ionization losses. Sunlight shadowing, separation of the vapor from the dust grains, dust thermodynamics and different impact plume models are considered.

Keywords: Collisionless atmosphere, exosphere, lunar atmosphere, lunar impact.
PACS: 96.20.-n, 96.20.Ka, 96.25.pq, 96.15.Qr, 96.15. St

INTRODUCTION

At present the Moon has no substantial atmosphere: the gravitational field is too weak, the daytime surface temperature too great, and exposure to solar wind and radiation too high, to maintain anything but a thin exosphere. Yet data from the Clementine mission [1] may indicate the presence of water ice in permanently shaded craters – "cold traps" – in the lunar South polar region. The interpretation of that data remains contentious, however [2,3,4]. The possibility of such deposits was first discussed by Watson, et al. [5] and subsequently elaborated upon by Arnold [6], Lanzerotti and Brown [7], Morgan and Shemansky [8] and Hodges [9], among others. The results from the Lunar Prospector (LP) mission appear to provide an even stronger case that there exists water near both poles [10,11]. The ice which may have been discovered by LP appears to be distributed widely but in a patchy manner and appears to be gardened into the regolith (soil) at a 1.5 ± 0.8% mixing ratio [12]or as patchy sheets of fairly pure ice overlaid by several centimeters of soil. Yet the thermal neutron data of Prospector do not guarantee the presence of water ice: the results could simply indicate hydrogen in some other form [13]. In addition, recent Arecibo radar results [14,15] show that both permanently shadowed and partially lit areas at the South pole have similar polarization properties so water ice may only be present as disseminated grains in these regions. Interpretations of Clementine photographic data clearly indicate the presence of permanently shadowed regions near the lunar poles [16] and the Goldstone radar results [17] provide precise topographic maps of the polar regions.

When the LP mission was completed, we attempted to use the spacecraft as a surface impactor in a cold trap to excavate a small amount of volatile material and make it briefly visible above the lunar surface [18]. This was, admittedly, an experiment having a low probability of success because of the low impact energy, poor trajectory control, extremely shallow impact angle and possibility only for Earth-based and Earth-orbiting observations. We attempted to observe a vapor plume of OH in its 3085 Å ultraviolet band with several telescopes while other observers looked for a wide range of other species. Unfortunately, nothing was found [19]. When the Lunar Reconnaissance Orbiter was moved to a larger Atlas 5 launch vehicle in 2006, NASA quickly developed a small

CP1084, *Rarefied Gas Dynamics: 26th International Symposium,* edited by T. Abe

lunar mission to make use of the 1000 kg extra launch mass available and the Lunar Crater Observation and Sensing Satellite (LCROSS, NASA Ames) was chosen. LCROSS will launch in November or December 2008 and in spring 2009 will impact in a south-polar crater. As described below, we model the mass and temperature distributions of lofted grains and the water and OH vapor evolved from those grains as seen from Earth and from the chaser spacecraft after impact.

The modeling of the LCROSS impact contains improvements in the physical representation since the LP studies. In particular, we model how vapor is released from the soil and what effects the initial debris spray cone assumptions have on the results. We have also improved the modeling of the terrain to accommodate viewing geometries and illumination.

We divide the possible sources of vapor into two categories: (i) vapor arising from the debris grains containing traces of water ice that are lofted by the impact into sunlight and warmed enough to sublimate off some water vapor and (ii) material that was warmed by the kinetic energy of the impact and forms a residue in the impact crater. This later source is the more uncertain of the two since it is not clear how much material is warmed, to what temperature it was heated, and whether it was on the surface or buried. This warm soil source was, however, the presumed vapor origin for the LP impact models. Instead, we here concentrate on the sun-warmed dust grains as the H_2O source and break the problem into the following pieces. We first model the motions of the grains. We then model each grain's temperature as it leaves (or not) the crater shadow. Warm grains create a spray of H_2O molecules that, in turn, produce OH radicals and together these two species move ballistically and scatter off the surface until they are lost.

Impact Model as the Initial Condition. The simulation of the actual spacecraft impact at ≈ 2.5 km/s and the crater formation is a difficult problem because of the details of the spacecraft structure and the poor knowledge of the soil mechanics. We do not do that. The best current estimate based on computer simulations and hypervelocity impact experiments of low density pellets into sand targets is that the lead vehicle will displace $O(10^6)$ kg of soil and produce a crater final radius of about 11m (Don Korycansky, private communication). Cintala, Berthoud, and Horz (CBH) [20] developed empirical models of the debris cone velocity field due to hypervelocity impacts. In their model, a particle's speed depends on how far it was from the actual impact point with particles initially near the center moving the fastest. We use their model in an acceptance/rejection scheme to determine the initial speed of the particles depending on where they originated in an 11m crater. Exponentially few particles end up with very large speeds and we truncate the maximum permitted speed at 800m/s (Peter Schultz, private communication). CBH also point out that for a range of impact conditions, the debris forms a cone with a nearly 45° angle to the surface; so our initial grain motion is inclined at 45°. This produces the expected "inverted lampshade" debris curtain.

Molecular Motion. Water molecules sublime off the grains as they move. The released water molecules may be observed as they fall and possibly scatter off the surface. When they contact the lunar surface, they have a residence time ($=5\times10^{-13}e^{4185/T_{surf}}$ s) depending on the local surface temperature [21][1]. While aloft and in sunlight, molecules following their elliptic trajectories may photodissociate to OH+H (time scale 8.3×10^4 s) or photoionize (time scale 2.45×10^6 s) and be lost. Atomic hydrogen is ignored. The OH is tracked separately from the H_2O and, for lack of better information, it is assumed to interact with the surface just like the H_2O (even though it is a radical and thus fairly reactive). The OH molecules fluoresce at 3085 Å when they are in sunlight. The gas and dust plume is modeled as optically thin and collisionless. Two views of the event are of most interest: the view from the chaser spacecraft that will be nearly over the south pole and the view from Earth (and Hubble Space Telescope -HST- since it is in a low Earth orbit). Particle motion is computed with a simple predictor-corrector approach in a central gravitational force field with a small (0.1 s) time step for early times and 1 s later. This molecular motion model is nearly the same as that described in Goldstein et al. [22].

Grain model. We assume that the scattered regolith grains are of uniform size and material. Kring [23], in his studies of lunar samples, suggests an average particle size of 70 μm. The particle emissivity is taken to be 0.5 and density as 3100kg/m^3. The specific heat of lunar samples over the present temperature range of interest is well fit by $C_p[J/kg-K] = 51.25 + 2.25\,T[K]$ [24]. Grain temperature is computed individually for each grain

[1] This is a crude approximation, at best, because it is based on residence times of water molecules on water ice and the lunar surface outside of the cold traps is probably completely free of pre-existing water.

depending on the illumination it is exposed to and its gray body emission ($\varepsilon\sigma T^4$). We assume that the grains are made of 1% water ice by mass and this ice does not alter the base thermal or optical properties. Our most important results are for water and OH column densities and these would simply scale linearly with the assumed initial water mass fraction of the grains.

Molecule Sources and Sinks. Water molecules sublimate off the regolith grains at a rate based on a vapor pressure suitable for the low temperatures of interest [25]:

$$P_v[Pa] = \left[3.712\times10^{12} - 1.326\times10^{8}T_{part} - 3.423\times10^{6}T_{part}^{2}\right] e^{-6150/T_{part}},$$

with T_{part} in K. This sublimation rate assumes the water lies close to the grain surface and diffusion time through the grain is negligible. Water molecules are lost and OH radicals are created by photodissociation. Molecules which are ionized are assumed to be lost as they are swept away by the solar wind. The surface temperature model assumes the sunlit surface is in radiative equilibrium, the day side is 370 K, the night side is at 120 K and the floors of the several craters modeled are at 90 K. Both H_2O and OH molecules can be lost, either temporarily or permanently, by condensation on a cool or cold surface depending on the local residence time. Figure 1 is a schematic view of some of the processes involved.

Detailed Geometry Model. The lunar surface is covered with a 1200x1200 grid and permanently shadowed craters are identified from radar and photograph data [14,15]. Crater rims are modeled as roughly cylindrical volumes extending some height above the surface of the Moon, in this case 2km. The height to which dust grains must rise to reach sunlight can vary by a large percentage of the crater's rim height depending on time of month, year, and location of impact within the crater. Our model accounts for these illumination variations through the influence of two phenomena - the rotation of the Moon about its polar axis and the 1.56° tilt of that axis with respect to the ecliptic plane. The height to sunlight directly above the impact point is assumed to be the height of shadow over the entire permanently shadowed region, which is an acceptable approximation as the debris plume sees a sun altitude error of only order 10m.

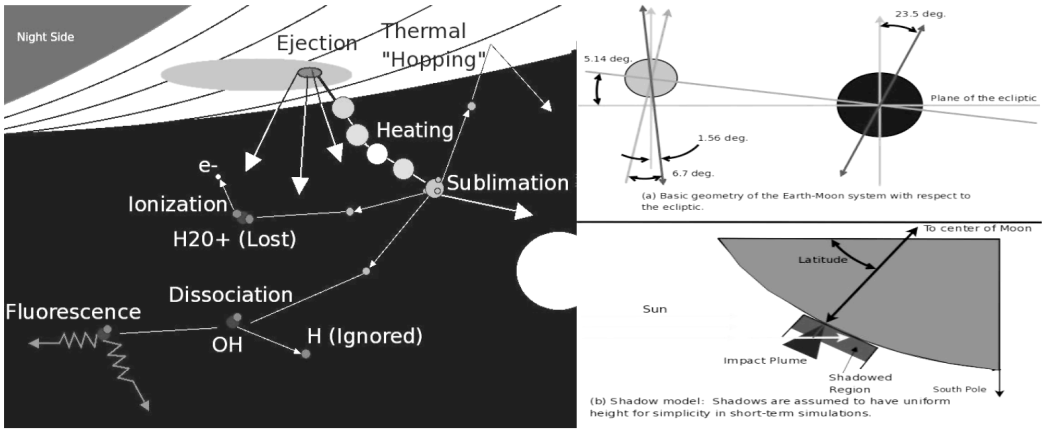

FIGURE 1: Schematic view of physical processes involved in molecular motion and (on the right) the geometric parameters involved in viewing the impact and the rise of the plume out of shadow.

RESULTS

Figure 2 illustrates a time sequence of the modeled line of sight water column density (in #/m^2) as seen from Earth for an impact near full moon. The impact point is chosen to be at –88.1° lat., 44.9° lon., in the 2 km deep Shoemaker crater. From this particular view, the impact site is just beyond the limb. The plume itself is seen to rise, spread and begin to collapse over the 1.5 minutes of the simulation. Of the 10^6 kg of soil presumed to be displaced by the impact, only ~19,000 kg of that ever rises high enough to be exposed to sunlight. From those sun-warmed grains, a net of ~180 kg of water vapor is sublimated of which 0.33 kg of OH is produced after five minutes. Figure 3 presents the expected dust grain column density for comparison. Notice how it differs from the water molecule plume shape because the grains follow a ballistic trajectory from the impact point while the molecules originate from the grains moving in sunlight. Figure 4 shows the projected temperature of the grains in the plume. There is little variation across the plume because most of the grains were in sunlight for about the

same amount of time. By the end of a minute, the small 70 μm grains have reached a radiative equilibrium temperature of about 270 K. The grain column density and temperature figures are provided as they can be used to estimate the UV and IR light scattered and emitted by the grain component that must be distinguished from the H_2O and OH components. The OH component is seen in figure 5. The OH plume shape reflects that of the water molecule plume. At these early times, few of the molecules seen have been in contact with the surface outside of the crater so the figures do not represent the uncertainty in the gas surface interaction. The OH signal reflects a balance of several effects: the increase with time in the number of source H_2O molecules due to warming of the dust grains, the progressive photodissociation of exposed H_2O molecules in sunlight, the geometric spreading of the plume and ultimately the loss of fluorescing OH molecules as they fall back into shadow.

Figure 6 presents the H_2O line of sight column density as seen from directly over the South pole in a manner analogous to what the following chaser spacecraft could perceive. The peak densities occur against the dark background of the crater floor. Few (only 1.25 percent) of the water molecules released from the grains actually make it beyond the crater rim to strike a warm lunar surface. Such molecules, once re-emitted with a surface-temperature dependent velocity, can hop about until they land in a shadowed region. These molecules form a thin transient exosphere, which may also be detectable. It should be noted, however, that the fraction of water molecules leaving the crater is strongly affected by the location of the impact within the target crater. Our example figures put the impact in the center of the crater.

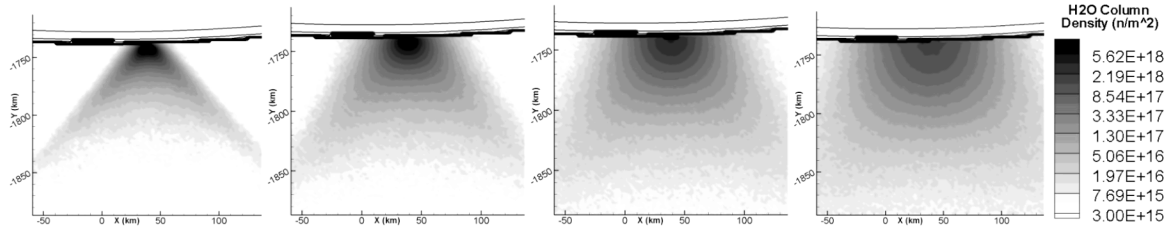

FIGURE 2: Earth view of LCROSS impact as seen in water vapor line of sight column density (#/m^2) at 25, 49, 73 and 97 seconds post impact. Axes are labeled in kilometers. Notice how the plume shape evolves from the "lampshade" when the water molecules are still largely moving with the dust grains to a more hemispherical profile as the thermal velocity of the molecules carries them away from the dust. The lunar limb is the thick nearly horizontal line while other lines indicate contours of lunar surface temperature.

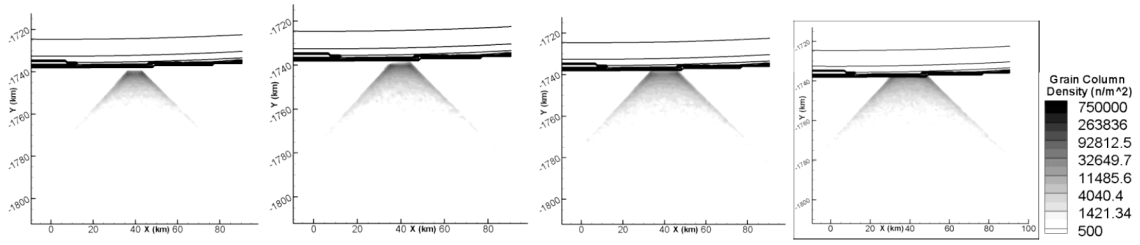

FIGURE 3: Dust grain column density at times corresponding to those in Fig.2. The grains move ballistically and hence produce a clear "lampshade" that spreads laterally near the base.

Perhaps most important will be modeling time-averaged observations. That is, the flows of gas and dust are fast and using a finite shutter speed blurs the observation. This is good in the sense of having a larger image to observe but bad in terms of a reduced peak photon count on a single pixel. In figure 7 contours of column density are shown averaged over the period from 25 to 97 seconds. These contours may be used to guide the exposure time and position of the HST STIS spectrograph with the 52 arc second slit and the McDonald Observatory long slit spectrograph (≅ 140 arc seconds). There are expected to be substantial areas in which the OH intensity exceeds the ~100 Rayleigh threshold that HST could detect. However, it will remain difficult to observe such an extremely diffuse plume as it rises out of the crater, especially with the bright

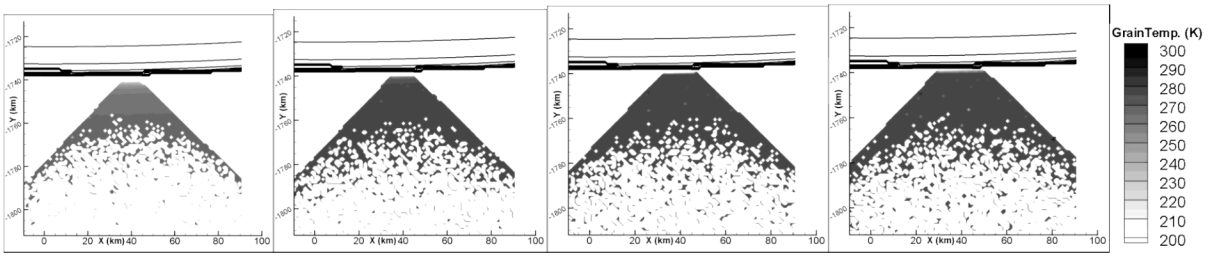

FIGURE 4: Grain temperatures at early times of 7, 19, 31 and 43sec. The first grains that rise into sunlight do, in fact, warm more quickly but after about half a minute most of the grains have nearly reached a radiative equilibrium temperature of about 270K.

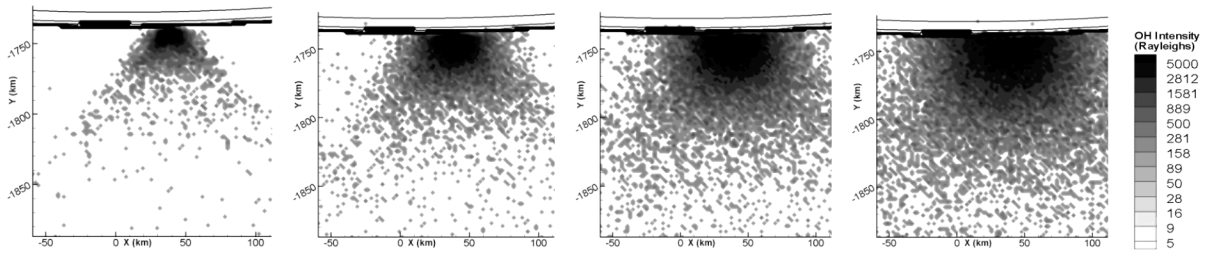

FIGURE 5: OH intensity in Rayleighs, in the 3085 Å band, from an Earth view at times corresponding to Fig. 1.

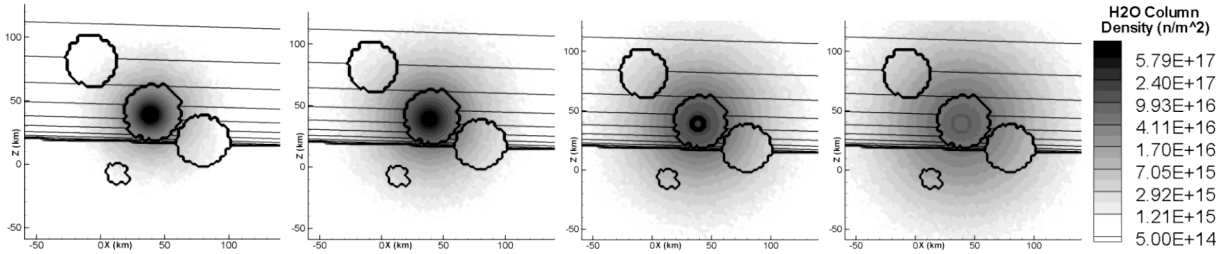

FIGURE 6: Water column density of aloft molecules as seen from over the south pole at times corresponding to those in Fig. 1. Note how the plume fringes have expanded beyond the crater edge even at 25 sec. Lines are again lunar surface temperature contours and indicate where the terminator is as well as outline four cold trap craters.

lunar disk contaminating the spectrum. Such simulations are now being run to aid in the planning for telescopic observations, e.g., exposure times, whether the STIS slit should be oriented vertically or horizontally, or whether to sweep the slit across the field. If the STIS slit is aligned vertically, one could eliminate surface scattering more readily at a few km from the surface as was shown by Barker et al. [19]. On the other hand, the expected OH brightness drops rapidly with altitude and an unfortunate streakiness or non-axisymmetry in the plume could render a portion of the plume under observation relatively dark. If one were to align the slit parallel to the lunar surface and compare pre-impact calibration spectra to post-impact spectra at, say, three different altitudes of 5 km, 10km and 20km one has a several chances of catching the brightest OH signal along the edge of the 'lamp shade'. However, HST pointing accuracy could lead to large uncertainty in scattered surface light.

Finally, where does the water end up? After 30 minutes the water molecules not still bouncing around are nearly all stuck on the night side of the Moon or in one of the permanently shadowed cold traps (Figure 8). In particular, most of the trapped water ends up back in Shoemaker crater. The kinetic energy of the impact is not sufficient to loft much water beyond its original crater boundary.

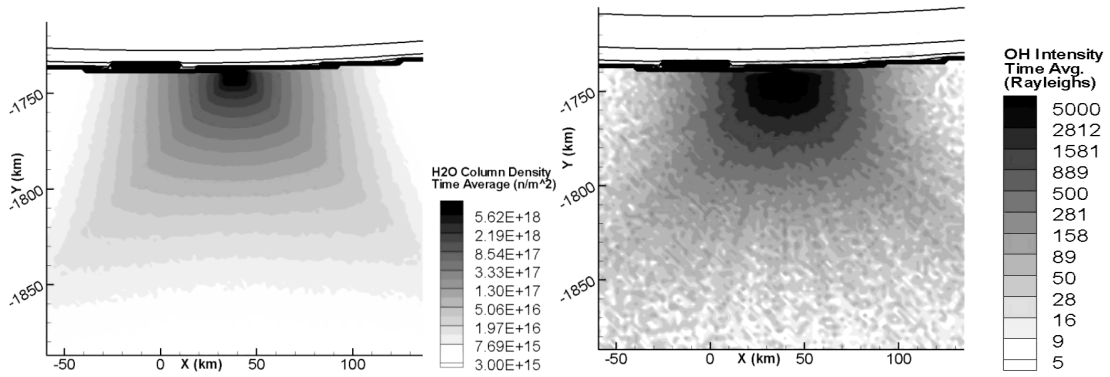

FIGURE 7: Time averaged column density of water and OH brightness averaged over the time 25 to 97 seconds. The predicted brightness in the OH (A-X) (0,0) band is in solar fluorescence at 3085 Å (brightness = (OH#/cm^2) 2.78×10^{-9}).

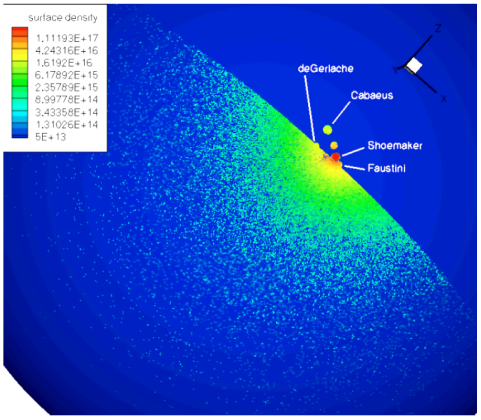

FIGURE 8: View from over the south pole showing the number density of water molecules stuck on the surface after 30 minutes of simulation. Note how particles accumulate in craters (mostly Shoemaker) and on the night side of the Moon.

ACKNOWLEDGEMENTS

This work was supported in part by NASA grants NNG04GQ66G and NNX08AZ42A

REFERENCES

1. Nozette, S. Lichtenberg, C. L., Spudis, P., Bonner, R., Ort, W., Malaret, E., Robinson, M. and Shoemaker, E. M., 1996. *Science*, vol. 274, 29 Nov..
2. Stacy, N. J. S., Campbell, D. B., and Ford, P. G., 1997. *Science*, 276, pp. 1527-1530.
3. Simpson, R. A. and Tyler, G. L., 1999. *J. Geophys. Res*, vol. 104, No. E2, pp. 3845-3862.
4. McConnochie, T. H., Buratti, B. J., Hillier, J. K., and Tryka, K. A., 2002. *Icarus* vol. 156, pp. 335-351.
5. Watson, K. Murray, B. and Brown, H. 1961. *J. Geophysical Res*, vol. 66, pp. 3303-3046, Sept..
6. Arnold, J. R., 1979. *J. Geophysical Res*., vol. 84, No. B10, Sept. 10.
7. Lanzerotti, L. J. and Brown, W. L, 1981. *J. Geophysical Res*, vol. 86, No. B5, pp. 3949-3950, May 10.
8. Morgan, T. H. and Shemansky, D. E, 1991. *J. Geophysical Res*, vol. 96, No. A2, pp 1351-1367, Feb. 1.
9. Hodges, R. R. 1991. *Geophysical Res. Letters*, vol. 18, No. 11, pp 2113-2116, Nov..
10. Feldman, W. C., Maurice, S., Binder, A., Barraclough, B. L., Elphic, R. C., and Lawrence, D. J., 1998. *Science*, **281**, 1496--1500.
11. Lawrence, D. J., et al., 2006. *J. Geophys. Res*. vol. 111, E08001.
12. Feldman, W. C., Lawrence, D. J., Elphic, R. C., Barraclough, B. L., Maurice, S., Genetay, I, and Binder, A., 2000. *J. Geophys. Res*., Vol. 105, No. E2, pp. 4175-4195.
13. Hodges, R. R. 2002. *J. Geophysical Res*, vol. 107, no. E2.
14. Campbell, B. A., and Campbell, D. B., 2006a. *Icarus* vol. 180, pp. 1-7.
15. Campbell, D. B., Campbell, B. A., Carter, L. M., Margot, J.-L., and Stacy, N, J., 2006b. *Nature*, vol. 443, pp. 835-837.
16. Bussey, D. B. J. , Spudis, P. D. , Robinson, M. S., 1999. *Geophys. Res. Let.* Vol. 26 , No. 9 , p. 1187.
17. Margot, J. L., Campbell, D. B., Jurgens, R. F., and Slade, M. A., 1999. *Science*, Vol. 284, pp.1658-1660.
18. Goldstein, D. B., R. S. Nerem, E. S. Barker, J. V. Austin, A. Binder, and W. Feldman, 1999. *Geophys. Res. Let*., **26**, pp.1653-1656.
19. Barker, E. and 38 others, 1999. BAAS, **31**, No. 5, pp 1583.
20. Cintala, Berthoud, Horz, 1999. *Meteoritics and Planetary Science*, Vol 34, pp. 605-623.
21. Sandford, S. A. and Allamandola, L. J. 1990. *Icarus*, **87**.
22. Goldstein, D., B., Stern, S. A., Crider, D. H., Gladstone, G. R., Durda, D., D., Asphaug, E., Larignon, B., Varghese, P. L., and Trafton, L. M, 2007. In *Rarefied Gas Dynamics,* Proceedings of the 25th International Symposium on Rarefied Gas Dynamics, ed., M. Ivanov & A. Rebrov, Publishing House of the Siberian Branch of the Russian Academy of Sciences, Novosibirsk, 2007.
23. Kring, 2006. Powerpoint presentation.
24. Horai, and Fujii, 1972. *Earth, Moon and Planets*, Vol 4., Numbers 3-4, Sept., pp 447-475.
25. Snowcrystals.com. See: www.its.caltech.edu/~atomic/snowcrystals/ice/ice.htm